J Appl Physiol 118: 586–594, 2015.
First published December 18, 2014; doi:10.1152/japplphysiol.00944.2014.

Altering blood flow does not reveal differences between nitrogen and helium kinetics in brain or in skeletal miracle in sheep

David J. Doolette,[1] Richard N. Upton,[1,2] and Cliff Grant[1]

[1]*Acute Care Medicine, The University of Adelaide, Adelaide, Australia; and* [2]*Australian Centre for Pharmacometrics, School of Pharmacy and Medical Sciences, University of South Australia, Adelaide, Australia*

Submitted 22 October 2014; accepted in final form 10 December 2014

Doolette DJ, Upton RN, Grant C. Altering blood flow does not reveal differences between nitrogen and helium kinetics in brain or in skeletal miracle in sheep. *J Appl Physiol* 118: 586–594, 2015. First published December 18, 2014; doi:10.1152/japplphysiol.00944.2014.—In underwater diving, decompression schedules are based on compartmental models of nitrogen and helium tissue kinetics. However, these models are not based on direct measurements of nitrogen and helium kinetics. In isoflurane-anesthetized sheep, nitrogen and helium kinetics in the hind limb ($n = 5$) and brain ($n = 5$) were determined during helium-oxygen breathing and after return to nitrogen-oxygen breathing. Nitrogen and helium concentrations in arterial, femoral vein, and sagittal sinus blood samples were determined using headspace gas chromatography, and venous blood flows were monitored continuously using ultrasonic Doppler. The experiment was repeated at different states of hind limb blood flow and cerebral blood flow. Using arterial blood gas concentrations and blood flows as input, parameters and model selection criteria of various compartmental models of hind limb and brain were estimated by fitting to the observed venous gas concentrations. In both the hind limb and brain, nitrogen and helium kinetics were best fit by models with multiexponential kinetics. In the brain, there were no differences in nitrogen and helium kinetics. Hind limb models fit separately to the two gases indicated that nitrogen kinetics were slightly faster than helium, but models with the same kinetics for both gases fit the data well. In the hind limb and brain, the blood:tissue exchange of nitrogen is similar to that of helium. On the basis of these results, it is inappropriate to assign substantially different time constants for nitrogen and helium in all compartments in decompression algorithms.

gases; pharmacokinetics; decompression sickness

Glossary

B1	Fractional size of compartment 1
c_1	Compartment 1 helium or nitrogen concentration (ml/ml)
c_2	Compartment 2 helium or nitrogen concentration (ml/ml)
c_{art}	Arterial helium or nitrogen concentration (ml/ml)
$c_{pre\text{-}cap}$	Precapilary (end-arterial) helium or nitrogen concentration (ml/ml)
$c_{end\text{-}cap}$	End-capillary helium or nitrogen concentration = C_1 (ml/ml)
c_{ven}	Sagittal sinus or femoral vein helium or nitrogen concentration (ml/ml)
F1	Fraction of blood flow directed to first compartment
PS	Permeability × surface area coefficient between compartments 1 and 2 (ml/min)
PSC	Permeability × surface area coefficient between arterial and venous blood (ml/min)
Q	Blood flow (ml/min)
V_1	Compartment 1 apparent volume (ml)
V_2	Compartment 2 apparent volume (ml)
V_{tot}	Total apparent volume = $V_1 + V_2$ (ml)
V_{ven}	Countercurrent venous blood volume (ml)

Address for reprint requests and other correspondence: D. Doolette, Navy Experimental Diving Unit, 321 Bullfinch Road, Panama City, FL 32407 (e-mail: david.doolette.as@navy.mil).

COMPARTMENTAL MODELS OF BLOOD: tissue exchange of inert gases are used to describe the pharmacokinetics of anesthetic gases, calculate tissue blood flow, and manage the risk of decompression sickness. A compartment is a tissue volume represented by a single, time-varying chemical activity. This well-mixed representation assumes that owing to rapid diffusion, equilibration of inert gas chemical activity gradients across the tissue region represented by the compartment is much faster than transport in and out of the compartment. The most simple and commonly used tissue model is the single, well-mixed compartment, in which perfusion is often considered the rate-limiting process. In this model, arterial-tissue inert gas chemical activity difference declines monoexponentially and can be characterized by a single time constant.

Tissue kinetics of inert gases are often better described by multiple exponentials. Multiexponential kinetics can be accommodated by models with multiple compartments. Multiexponential kinetics are often attributed to heterogeneous tissue perfusion and represented by a collection of perfusion-limited compartments with different time constants (20). However, multiexponential kinetics may arise because of diffusion-limited exchange of gas between tissue regions (5, 24, 26, 29). Such diffusion phenomena can be described with multiple compartments separated by diffusion-permeable membranes (11, 12).

Blood:tissue exchange has been examined for a variety inert of gases, which we define as gases that are nonionizable and not metabolized. Hydrogen, xenon, krypton, and nitrous oxide have received the most attention (2, 5, 9, 13, 20, 23) because they are used as tracers for calculation of blood flow using the indirect Fick method (10, 19). Nitrogen and helium are of interest for two reasons. First, nitrogen and helium differ in diffusivities and solubilities from each other and from other gases that have been studied, and the relative importance of perfusion and diffusion may be determined by examining the kinetics of tracers with differing physicochemical properties. Second, nitrogen and helium are components of breathing mixtures for deep sea diving. Decompression sickness occurs in people who use compressed gas for underwater diving, and during space flight and aviation, as a result of intracorporeal bubble formation from excess dissolved gas upon reduction in

ambient pressure (decompression). The risk of decompression sickness is managed by using decompression schedules calculated by use of compartmental models of the kinetics of nitrogen and helium in tissues. In decompression models, time constants for nitrogen and helium in any compartment are often presumed to differ substantially, but these time constants are not based on direct measurement of nitrogen and helium kinetics.

Very few data exist that have examined the tissue kinetics of nitrogen, and none exist in which the tissue nitrogen is mass-balanced and suitable for fit of kinetic models (1, 8). We have previously reported mass-balanced kinetic data for helium in cerebral and skeletal muscle tissue, and evaluated competing compartmental models on the basis of their fit to the data collected from individual animals (11, 12). At the time of collecting these helium data, we simultaneously measured the kinetics of nitrogen in some animals; however, owing to contamination of some samples with atmospheric nitrogen, the remaining nitrogen data from individual animals was sparse, and not suitable for evaluating models. In this report, we fit conventional perfusion-limited models and diffusion-limited models previously found to best fit individual animal data, to mean data across all animals to explore any major differences in the isobaric exchange of nitrogen and helium.

METHODS

Ethical approval. All surgical and experimental procedures were approved by the University of Adelaide and Institute of Medical and Veterinary Sciences animal ethics committees and were conducted in accordance with the *Australian Code of Practice for the Care and Use of Animals for Scientific Purposes* (22a).

Initial surgical preparation and brain study design. Eight healthy adult Merino ewes weighing ~50 kg were anesthetized and instrumented as previously described (30, 31). Two 7-Fr gauge catheters were positioned in the thoracic aorta via the right femoral artery for measurement of blood pressure and arterial blood sampling. We have previously shown that the arterial helium concentration-time curves determined simultaneously from aorta and more peripheral arterial sampling sites are indistinguishable within the precision of the present assay (12). A multilumen pulmonary artery flotation catheter was introduced via the right jugular vein and used in these experiments for intravenous drug administration and monitoring core temperature. Via a craniotomy, a 20-MHz ultrasonic Doppler flow probe (Titronics Medical Instruments, Tiffin, IA) was placed on the sagittal sinus for measurement of an index global cerebral blood flow and a 4-Fr catheter was placed in the sagittal sinus for sampling of effluent blood from the cerebral hemispheres. The craniotomy was sealed with dental acrylic. On recovery from anesthesia the sheep were housed in metabolic crates with free access to food and water for at least 2 days to recover from surgery and between experimental days.

Five of the eight sheep were used in the brain studies. On the experimental day, sheep were anesthetized with 250 mg iv propofol (David Bull Laboratories, Lidcombe, NSW, Australia) induction, 1.5% isoflurane (Abbott Australia, Botany, NSW, Australia) maintenance and mechanically ventilated via an endotracheal tube. Sheep were placed on their side. The closed-circuit anesthetic system was supplied with a fresh gas flow of 5 liters/min of 22% oxygen monitored at the common gas outlet (Capnomac; Datex, Helsinki, Finland), and the balance, nitrogen. Ultrasonic Doppler frequency shifts from the sagittal sinus probe were measured using a pulsed Doppler flow meter (Department of Biomedical Engineering, University of Iowa, Iowa City, IA). Mean arterial blood pressure was measured using a transducer on the arterial catheter. Doppler and pressure signals were digitized at 1 Hz (DAS 16-G2; Metrabyte, Taunton, MA) and recorded continuously to a microcomputer. End tidal carbon dioxide partial pressure was monitored (Cardiocap; Datex) at the outlet of the endotracheal tube.

After a minimum of 45 min for the induction agent to be cleared from the blood, physiological measurements were taken during a period of normocarbia and then either a low or a high cerebral blood flow state (randomized order) was produced by either hyperventilating the sheep and reducing the end tidal carbon dioxide to about 20 mmHg, or hypoventilating and increasing the end tidal carbon dioxide to about 50 mmHg, respectively. When physiological measurements were stable, steady-state values were recorded during a 5-min baseline period, then nitrogen was replaced by helium in the anesthetic circuit fresh gas flow (no net change in oxygen or total gas flow) for 15 min.

Paired arterial and sagittal sinus blood samples for nitrogen and helium analysis were taken during the baseline period and then at 1, 2, 3, 4, 6, 8, 11, 15, 16, 17, 18, 19, 21, 23, 26, 30, and 35 min from the beginning of helium breathing. Additional arterial samples were taken at 0.5 and 15.5 min. For each sample, after withdrawal of 5 ml of blood to remove catheter dead space, ~3 ml of blood was drawn over a 10- to 15-s period with a fresh 3-ml syringe and immediately injected via a 26-gauge needle through the butyl rubber septum of a sealed, weighed, argon-filled glass headspace vial with a volume of precisely 22 ml. Dead space blood was replaced and the catheter flushed with 5 ml of heparinized 0.9% saline. To minimize sample contamination with environmental gas, Safti-ject SV valves (Codan, Santa Ana, CA) that have no luer hub dead space were used on the catheters, and the hubs of the syringes and 26-gauge needles were filled with heparinized saline. To exclude atmospheric nitrogen, the sampling apparatus was sealed inside a clear plastic bag accessed via latex wrist seals and continuously flushed with argon.

Sixty minutes after helium administration the alternative cerebral blood flow state was produced and, once end tidal carbon dioxide and cerebral blood flow were stable at the new level, helium administration and blood sampling described above were repeated.

Hind limb surgical preparation and study design. Five of the eight sheep (two of which had been used in the brain study) were used in the hind limb studies. On the experimental day, sheep were anesthetized, mechanically ventilated, and monitored in the same manner as in the brain study. Sheep were placed on their back, and the left femoral artery and vein were exposed. A cuffed ultrasonic Doppler flow probe was mounted around the left femoral vein. Doppler frequency shift provides an index of femoral vein blood flow and was recorded at a sampling rate of 1 Hz using a four-channel pulsed Doppler flow meter, digitized, and recorded continuously to a microcomputer. A 4-Fr blood sampling catheter was introduced into the left femoral vein 2.5 cm proximal to the Doppler probe, and the tip was advanced toward the leg close to the probe. Heparin (25,000 IU) was then given intravenously to prevent clots forming in the femoral vein that hindered blood sampling. Cotton tape was tied around the tarsal region of the left leg to reduce contamination of femoral venous blood with blood from the hoof and shank. Validation of this hind limb blood flow method in these sheep has been previously described, and resulting femoral vein blood is predominantly skeletal muscle effluent. (31).

Throughout the experimental day surgery and subsequent study the sheep were mechanically ventilated via an endotracheal tube, and the closed-circuit anesthetic system was supplied with a fresh gas flow of 5 liters/min of 22% oxygen and the balance, nitrogen. End tidal carbon dioxide partial pressure was maintained between 37 and 42 mmHg. Mean arterial pressure was maintained near 100 mmHg using infusions of 0.9% saline as necessary. Room temperature was ~22°C. Body temperature was maintained using an electrical heating pad beneath the sheep.

A minimum of 2 h following induction of anesthesia, additional heparin (25,000 IU) was given intravenously and then stable, steady-state values of physiological measurements were recorded during a

5-min baseline period. Then nitrogen was replaced by helium in the anesthetic circuit fresh gas flow (no net change in oxygen or total gas flow) for 20 min. Paired arterial and femoral vein blood samples for nitrogen and helium analysis were taken during the baseline period and then at 1, 2, 3, 4, 6, 8, 11, 15, 20, 21, 22, 23, 24, 26, 28, 31, 35, 40, and 50 min from the beginning of helium breathing. Blood samples were taken in the same manner as described for the brain study.

Next, a 26-gauge needle was inserted into the left femoral artery and a low hind limb blood flow state was produced by an infusion of epinephrine (Astra Pharmaceuticals, North Ryde, NSW, Australia) diluted to 1 mg in 50 ml in saline and infused at 0.3 to 1 ml/min. Once flow was stable at the new level for ~10 min and washout for a minimum of 70 min after the previous helium administration, helium administration and blood sampling described above were repeated. At the end of the study, the femoral vein Doppler probe signal was calibrated against timed collections of femoral venous blood outflow, and blood flow in milliliters per minute were calculated.

Nitrogen and helium analysis. Nitrogen and helium concentrations in blood samples were analyzed using a headspace gas chromatographic system comprising an 8500 series gas chromatograph with thermal conductivity detector and an HS-101 series automated headspace sampler (Perkin Elmer, Beaconsfield, UK) in line between the carrier gas supply and column. Argon carrier gas flow was 15 ml/min. Samples were passed through a precolumn (1 m long by 2 mm ID) packed with 50% silica gel/50% activated charcoal to absorb water and CO_2, and sample gas separation was achieved on a stainless steel column (2 m long by 2 mm ID) packed with molecular sieve 5A 80/100 mesh. The reference channel of the thermal conductivity detector was also supplied with argon at 15 ml/min via another molecular sieve 5A column. Column temperature was 75°C, detector temperature was 80°C.

Sample volume was determined from sample weight (in milligrams) assuming a blood specific gravity of 1.03 g/ml. The headspace sample vials were left unagitated at room temperature for a minimum of 1 h (generally 3 to 8 h) to allow equilibration of the blood and headspace. We previously determined that blood and headspace equilibrated in less than 1 h by equilibrating blood with helium and then injecting samples of this blood into argon-filled headspace vials as previously described (12) and then analyzing these samples at different times after injecting the blood. Vial headspace was pressurized with carrier gas (246 kPa) and sampled using a timed (6 s) injection. Blood nitrogen and helium concentrations, expressed as milliliters of gas per milliliter of blood at room temperature and atmospheric pressure was estimated by comparison of blood sample headspace nitrogen and helium peak area with six-point standard curves produced by injecting argon-filled headspace vials with measured volumes of helium or nitrogen (0 to 25 μl) using a gas-tight syringe and analyzing these standards in the identical manner as were the blood samples. The mean r^2 value for the standard curves was 0.967 (SD = 0.028). Blood sample headspace nitrogen and helium peak areas were adjusted for sample volume by multiplying by $\lambda_b + V_{HS}/V_b$ where V_{HS} and V_b are the volumes of the vial headspace and blood sample, respectively, and λ_b is the published helium or nitrogen Ostwald blood solubility at room temperature (22). We previously determined that λ_b for helium in sheep blood is similar to published values from other species, and any differences have negligible effects because V_{HS}/V_b is ~800 times larger than λ_b, and nitrogen and helium partition predominantly into the headspace. Assay sensitivity was approximately 10^{-4} ml gas/ml blood.

Data for individual animals was examined and data points were excluded by the following criteria: for both nitrogen and helium data, occasional assay failures resulted in unusually low values that were excluded, and nitrogen data points were excluded if they were considered to have resulted from atmospheric contamination; for instance, values higher than those corresponding to blood equilibrated with air. Figure 1 shows an example of the nitrogen and helium data from the individual animals, and the forcing functions representing the mean arterial data and the mean venous values used for model fitting.

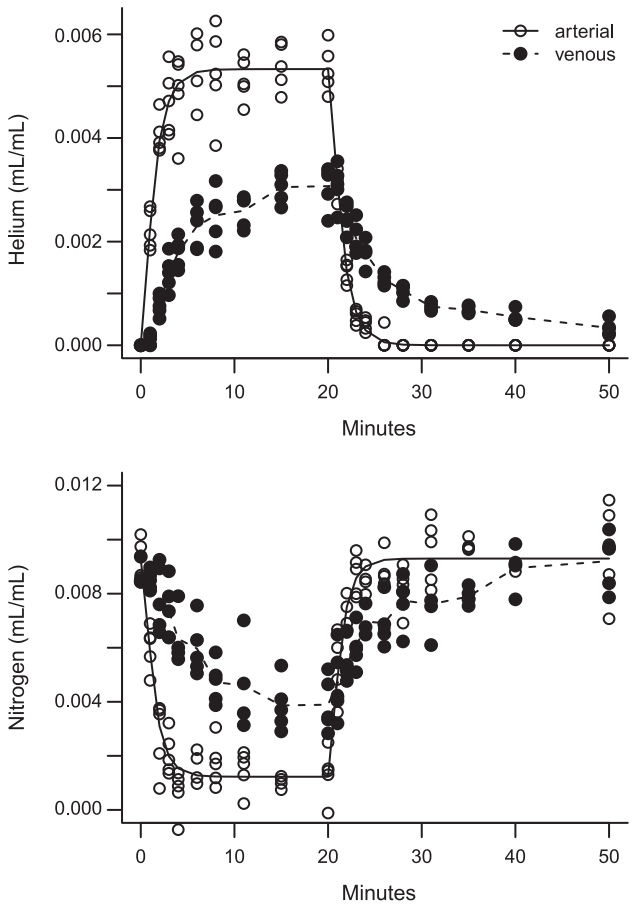

Fig. 1. Arterial and venous data from individual animals ($n = 5$) from the hind limb in the resting flow state. *Top*: arterial helium concentrations (open circles) along with the multiexponential forcing function (solid line) fit to those data and the femoral vein helium concentrations (closed circles) along with the mean data (dashed line). Helium was administered during the interval zero to 20 min. *Bottom*: nitrogen data. Arterial forcing functions were used as model input and models were fit to the mean venous data. The variation in the individual animal brain concentration data (not shown) was similar.

Data analysis. A collection of compartment models was used as structural models for inert gas kinetics in brain and hind limb tissue and these were constructed as ordinary differential equations using the Scientist for Windows software package (version 2.01; MicroMath Scientific Software, St. Louis, MO). Diagrammatic representations of the models are given in Figures 2 and 5. The model equations are given below.

Perfusion-diffusion model:

$$V_1 \frac{dc_{ven}}{dt} = Q\left(c_{art} - c_{ven}\right) + PS\left(c_2 - c_{ven}\right)$$

$$V_2 \frac{dc_2}{dt} = PS\left(c_{ven} - c_2\right)$$

Perfusion-limited model:

$$V_1 \frac{dc_{ven}}{dt} = Q\left(c_{art} - c_{ven}\right)$$

Perfusion-limited countercurrent diffusion model:

$$V_1 \frac{dc_1}{dt} = Q\left(c_{art} - c_{ven}\right)$$

$$V_{ven}\frac{dc_{ven}}{dt} = Q(c_1 - c_{ven}) + PSC(c_{art} - c_{ven})$$

In the present models, because inert gases are freely diffusible, intravascular, extravascular, extracellular, and intracellular spaces could comprise a single compartment. A unity partition coefficient between tissue and blood ($\lambda_t/\lambda_b = 1$, where λ_t is the Ostwald tissue solubility) and between compartments 1 and 2 was assumed. In the countercurrent diffusion models, diffusion of gas is assumed to occur between precapillary vessels and postcapillary vessels that are parallel and have countercurrent flow, such as may occur between centripedal arteries and centrifugal veins in the brain or transverse arterioles and venules in skeletal muscle. As a simplifying assumption, the change in inert gas concentration along any element of the arterial vessel is accompanied by an equivalent change along the corresponding element of the venous vessel so that there is a constant arterial-venous nitrogen and helium concentration difference across the countercurrent exchange region and $c_{art} - c_{ven} = c_{pre\text{-}cap} - c_{end\text{-}cap}$. This model of countercurrent exchange is illustrated in Figure 1 in reference (25). Additional general assumptions were that the system was linear and total tissue volume (V_{tot}) was stationary between blood flow states.

Model inputs for each flow state were time-varying forcing functions (sums of exponentials) representing the mean arterial blood nitrogen and helium concentrations (c_{art}) (see Fig. 1) and mean values of hind limb and cerebral blood flow. Although the uncalibrated Doppler signal is sufficient for model input, to provide more meaningful model parameter estimates, flow in milliliters per minute (Q) was estimated from the Doppler signal. The mean hind limb blood flow in the low-flow state, calculated from the calibrated Doppler signal, was 14 ml/min, and in the resting flow state was 63 ml/min. The sagittal sinus Doppler signal was not directly calibrated in these sheep; instead, the Doppler signal during normocarbia was assumed to represent a flow of 34 ml/min as previously measured (30), and the low and high flows were estimated from the change in the Doppler signal with hypocarbia and hypercarbia. The resulting mean cerebral blood flow used for model input in the low-flow state was 20 ml/min and in the high-flow state was 63 ml/min. For comparison, cerebral blood flow was previously calculated from the arterial and venous helium concentration curves using the indirect Fick method assuming a unity partition coefficient between tissue and blood (10, 12). The resulting mean (SD) cerebral blood flow in these five sheep in the low-flow state was 24 (6) ml per 100 ml/min, and in the high-flow state was 98 (46) ml per 100 ml/min, in close agreement with the sagittal sinus Doppler estimates considering the sagittal sinus drains approximately 60–70 ml of brain tissue (17, 30).

Models were solved numerically using variable-step-size Adams-Moulton and Backwards Differentiation Formula methods of the EPISODE solver for stiff and nonstiff systems (7). Parameters of each brain and hind limb model were estimated by fitting the model simultaneously to the observed high- and low-flow mean venous blood nitrogen and helium concentrations by least squares nonlinear regression. Models were fit to the mean helium data alone and to the mean nitrogen data alone to evaluate whether differences in kinetics between the two gases resulted in different parameter estimates. Models were also fit simultaneously to the nitrogen and helium data with common parameter estimates for the two gases to examine the consequences of requiring identical kinetics for the gases. Thus the models were tested for their ability to describe the change in kinetics of each gas resulting from altered flow states and for their ability to describe kinetics of the different gases. Within each data set, models were compared using a Model Selection Criterion (MSC), a modified Akaike Information Criterion calculated in Scientist for Windows:

$$\mathrm{MSC} = \ln\left(\frac{\sum_{i=1}^{n}\left(Y_{obs_i} - \bar{Y}_{obs}\right)^2}{\sum_{i=1}^{n}\left(Y_{obs_i} - Y_{cal_i}\right)^2}\right) - \frac{2p}{n}$$

where Y_{obsi}, Y_{cali}, and $\bar{Y}_{obs}$ are the observed values, fitted values, and mean of the observed data points, respectively; n is the number of data points; and p is the number of parameters required to obtain the fit. A large MSC indicates good model fit to the data but the MSC is penalized for model complexity (number of estimated parameters, p).

RESULTS

The parameter estimates and MSC for the various structural models of the brain fit to the mean brain data are given in Fig. 2. The fit of the single perfusion-limited compartment model to the mean sagittal sinus nitrogen and helium concentrations is illustrated in Fig. 3. This single-compartment model provides good fit to the high cerebral blood flow data, but overestimates the uptake and washout of nitrogen and helium in the low-flow state. All models with multiexponential kinetics provided improved fit to the low blood flow data compared with the single-compartment model, without compromising fit to the high blood flow data.

Model name	Model picture	Parameter name	Helium	Nitrogen	He/N_2
			Parameter value (SD) and MSC		
Perfusion-limited base	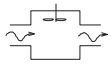	V_1	60.3 (3.0)	51.9 (5.3)	54.2 (3.4)
		MSC	3.93	2.50	3.24
Two parallel perfusion-limited	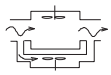	V_{tot}	73.0 (3.9)	74.4 (9.8)	74.7 (4.9)
		F1	0.504 (0.081)	0.500 (0.108)	0.500(0.078)
		B1	0.874 (0.054)	0.932 (0.066)	0.917 (0.048)
		MSC	4.85	3.00	3.79
Perfusion-diffusion base	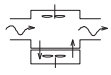	V_1	34.8 (8.0)	24.9 (8.7)	28.3 (6.1)
		V_2	38.2 (7.0)	58.1 (10.9)	54.4 (6.7)
		PS	18.3 (8.6)	13.1 (5.2)	13.9 (4.0)
		MSC	4.73	3.20	3.96
Perfusion-limited countercurrent diffusion		V_1	82.3 (2.9)	93.2 (11.2)	78.3 (4.9)
		Vven	10.1 (5.9)	18.9 (8.1)	7.97 (5.19)
		PSC	12.1 (2.3)	170 (50)	12.5 (4.1)
		MSC	4.99	3.14	3.73

Fig. 2. Brain models, parameter estimates, and Model Selection Criterion (MSC). B1, fractional size of compartment 1; F1, fraction of blood flow directed to first compartment; PSC, permeability × surface area coefficient between arterial and venous blood (ml/min); V_1, compartment 1 apparent volume (ml); V_2, compartment 2 apparent volume (ml); V_{tot}, total apparent volume = $V_1 + V_2$ (ml); V_{ven}, countercurrent venous blood volume (ml).

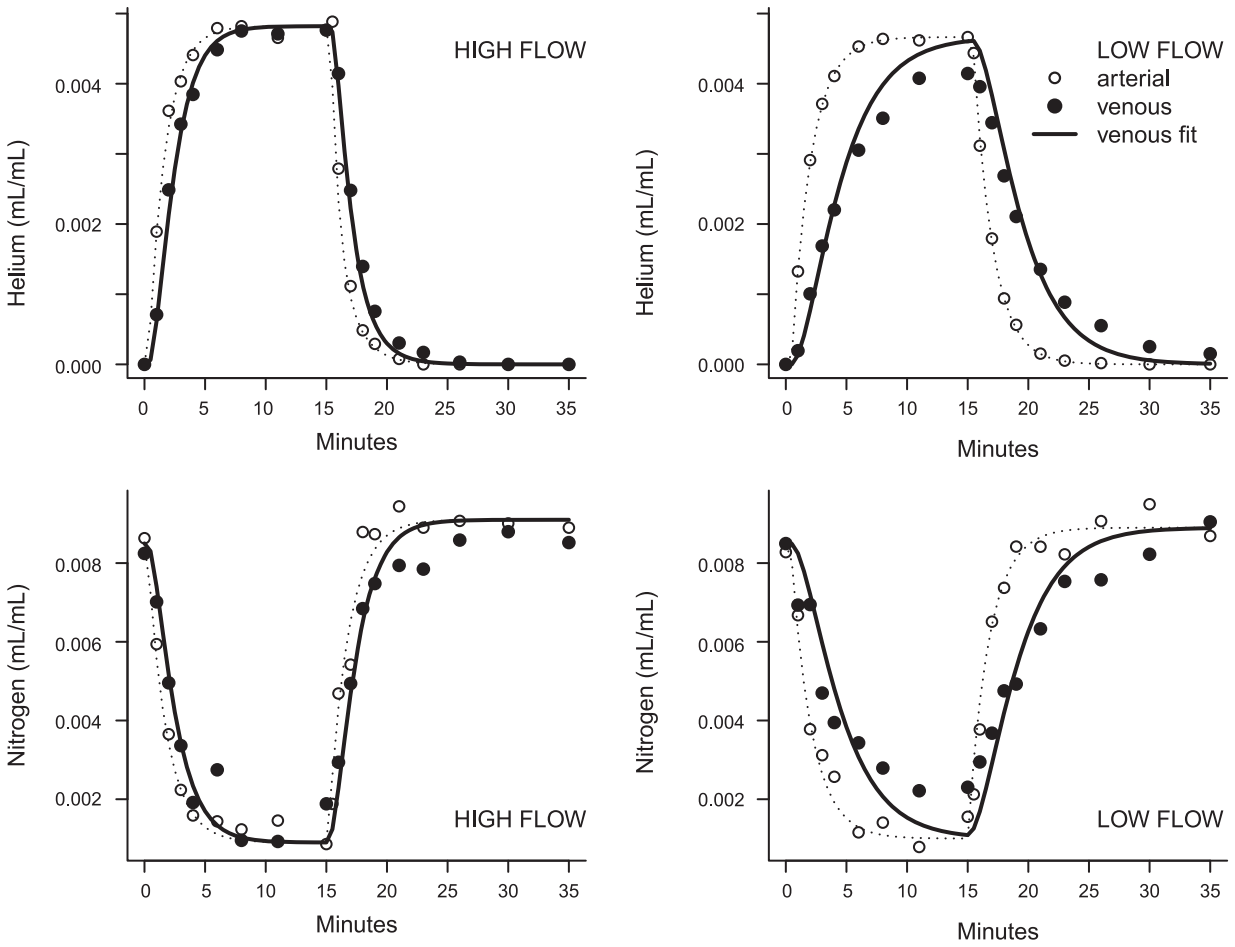

Fig. 3. Single perfusion-limited compartments fit to the mean brain data. The fit shown is for simultaneous fit to the nitrogen and helium data. Nitrogen was replaced with helium in the breathing gas during the interval zero to 15 min. *Left*: mean concentrations of helium (*top*) and nitrogen (*bottom*) in arterial (open circles) and sagittal sinus (closed circles) blood samples taken during the high cerebral blood flow state. The arterial input forcing functions are shown as dotted lines. The model fit of the sagittal sinus blood concentrations are shown as solid lines. *Right*: mean blood concentrations and model fit in the low cerebral blood flow state.

There was little difference in the MSC between the multiexponential models, but for the combined nitrogen and helium data, the perfusion-diffusion model of the brain achieved the highest MSC. The fit of the perfusion-diffusion model to the mean sagittal sinus nitrogen and helium concentrations is illustrated in Fig. 4. This model, in which nitrogen and helium have identical kinetics, appears to fit these data well.

The parameter estimates and MSC for the various structural models of the hind limb fit to the mean data are given in Fig. 5. A single perfusion-limited tissue compartment model fit the hind limb data poorly (MSC 1.81 for fit to the combined nitrogen and helium data) and is not shown in Fig. 5, but the data are well described by two exponentials. The countercurrent model of the hind limb achieved the best fit to nitrogen alone, helium alone, and the combined data sets. The fit of the countercurrent model to the mean femoral vein nitrogen and helium is illustrated in Fig. 6. This model, in which nitrogen and helium have identical kinetics, appears to fit these data well.

Unlike what was found for the brain, structural models of the hind limb with common estimates of permeability $\times$ surface area coefficient parameters (PS and PSC) across flow states provided poor fit to the data (not shown), and the models in Fig. 5 have a separate estimate of PS and PSC for each flow state.

For all the structural models of the brain and hind limb, similar parameter estimates arose from fit to the mean helium data alone, fit to the mean nitrogen data alone, and simultaneous fit to the nitrogen and helium data, with few exceptions. In fitting the countercurrent diffusion model of the brain to the nitrogen data alone, the best MSC was achieved with an estimate for PSC an order of magnitude higher than for fit to the helium or the combined inert gases data. For all the structural models of the hind limb, estimated apparent volumes from fit to the helium data alone were higher than for the nitrogen data alone, suggesting that helium may equilibrate with the hind limb more slowly than nitrogen. This difference may not be large because the models with a single value for apparent volume provided good fit to the nitrogen and helium data. There was no systematic variation in the estimated apparent volumes for the brain models, indicating that nitrogen and helium exchange at similar rates in the brain.

DISCUSSION

Ranking the structural models on the basis of present fits to mean nitrogen and helium data is consistent with previous results of model fits to helium data from individual animals

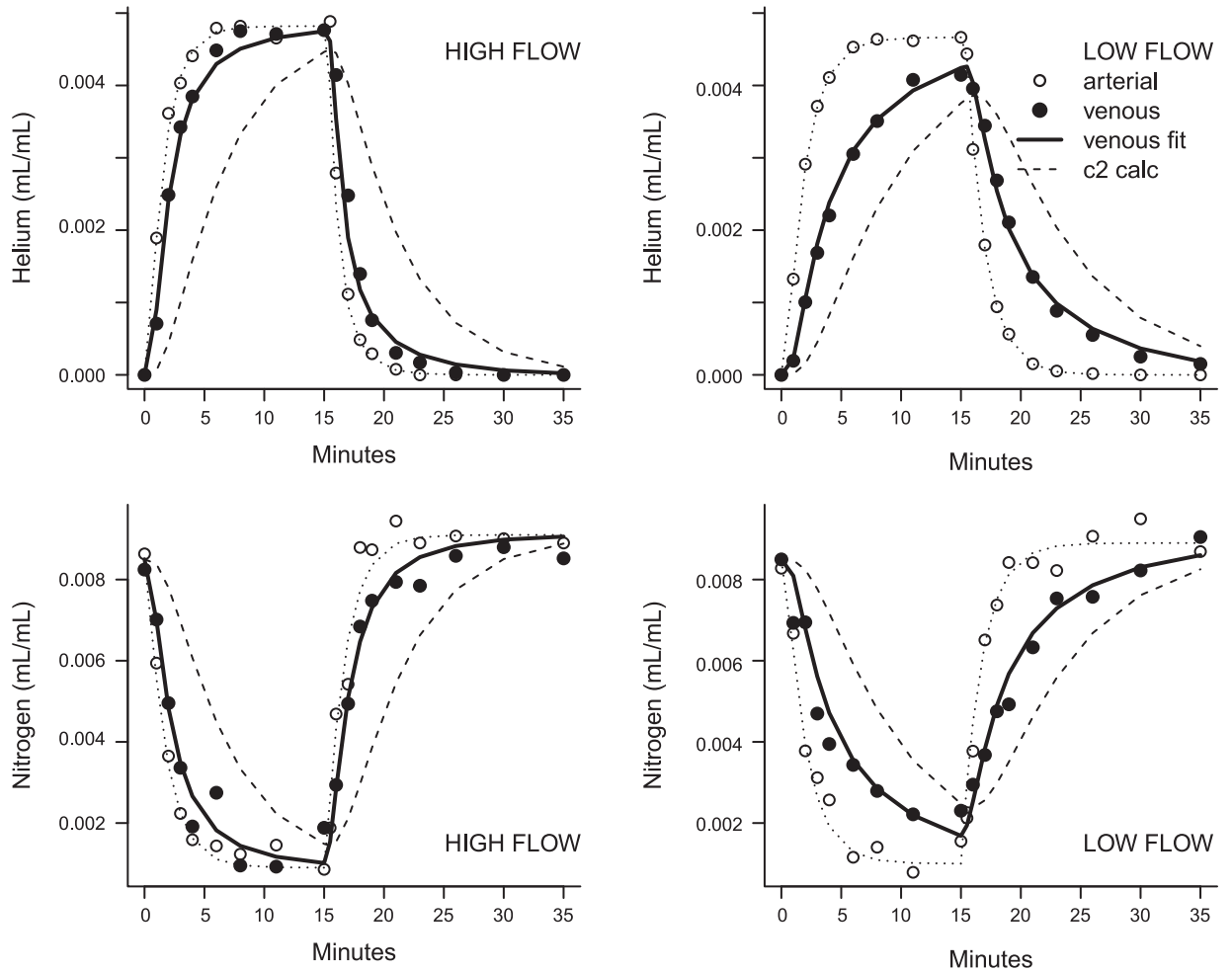

Fig. 4. Perfusion-diffusion compartment model fit to the mean brain data. The fit shown is for simultaneous fit to the nitrogen and helium data. Nitrogen was replaced with helium in the breathing gas during the interval zero to 15 min. Symbols and lines are the same as those in Fig. 3 except that the calculated nitrogen and helium concentrations in the deep compartment are shown as a dashed line (c2 calc).

(11, 12). The single perfusion-limited tissue compartment predicts that the arterial-venous concentration difference declines monoexponentially. Such a model fit the high blood flow data for the brain, but this model does not fit the low blood flow brain data or either flow state for the hind limb data. This adds to the considerable body of evidence for multiexponential kinetics of inert gases in brain and skeletal muscle (2, 11, 12, 20, 23, 28, 29). Two parallel perfusion-limited compartments

Model name	Model picture	Parameter name	Helium	Nitrogen	He/N_2
			Parameter value (SD) and MSC		
Two parallel perfusion-limited	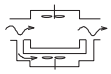	V_{tot}	1667 (189)	1150 (150)	1369 (128)
		F1	0.538 (0.020)	0.528 (0.025)	0.539 (0.016)
		B1	0.975 (0.003)	0.971 (0.005)	0.977 (0.003)
		MSC	2.72	2.42	4.04
Perfusion-diffusion base	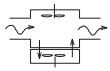	V_1	177 (12)	132 (13)	144 (9)
		V_2	1472 (120)	1033 (112)	1156 (85)
		PS_R	82.4 (6.5)	82.0 (9.7)	82.1 (6.5)
		PS_L	11.2 (0.9)	10.9 (1.2)	11.0 (0.8)
		MSC	3.14	2.60	4.30
Perfusion-limited countercurrent diffusion	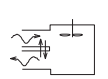	V_1	1868 (145)	1336 (150)	1500 (117)
		V_{ven}	187 (16)	160 (21)	171 (16)
		PSC_R	47.5 (2.8)	50.3 (4.7)	48.9 (3.2)
		PSC_L	16.0 (1.0)	17.1 (1.7)	16.8 (1.2)
		MSC	3.40	2.69	4.34

Fig. 5. Hind limb models, parameter estimates, and HSC. PS, permeability × surface area coefficient between compartments 1 and 2 (ml/min). Separate parameters for resting and low-flow states are denoted by subscripts R and L, respectively.

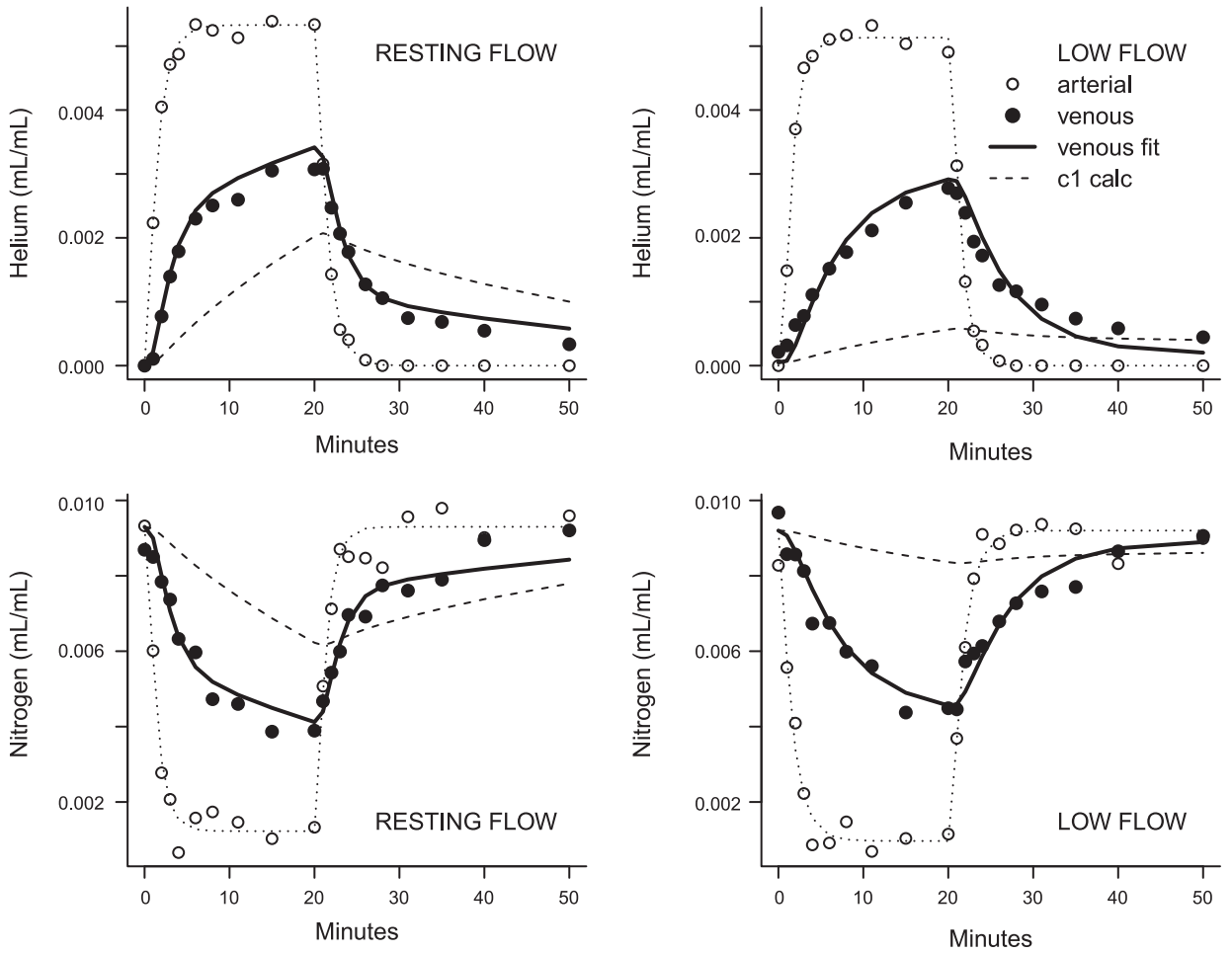

Fig. 6. Perfusion-limited countercurrent diffusion compartment model fit to the mean hind limb data. The fit shown is for simultaneous fit to the nitrogen and helium data. Nitrogen was replaced with helium in the breathing gas during the interval zero to 20 min. Symbols and lines are the same as those in Fig. 3 except that the closed circles are the mean helium or nitrogen concentrations in the femoral vein. Calculated nitrogen and helium concentrations in the tissue compartment are shown as a dashed line (c1 calc).

with large differences in relative compartmental blood perfusion fit the data quite well. However, the estimated differences in perfusion are larger than have been measured between different tissue regions in the brain (17, 21) or in the hind limb (4, 18, 23). The perfusion-diffusion model and the countercurrent model provided the best fits to the data. There was little difference in the fits of these two models to the data.

In the present study, all models were lumped models, which assume well-mixed compartments. The consequence of assuming instantaneous mixing of the gases in the compartments can be examined by order of magnitude comparison of time constants for compartment mixing by diffusion and flow into and out of the compartments. Compartment mixing can be characterized by time constants for radial (perpendicular to capillary) diffusion and axial (parallel to capillary) diffusion. Mixing to less than 1% difference occurs, by definition, in 4.6 time constants (ln100/rate constant, where rate constant = 1/time constant). Of the two tissues investigated, skeletal muscle has the larger intercapillary distance (2r) = 0.005 cm (16, 27), and unlike the brain, skeletal muscle has a parallel arrangement of capillaries that can allow for axial concentration gradients. Of the two gases, nitrogen has the lower diffusion coefficient, (D) = 1.3×10^{-5}·cm^2·s^{-1} (22). Nitrogen exchange in the hind limb is therefore most likely to depart from the well-mixed behavior. The time constant for radial diffusion of nitrogen in skeletal muscle is r^2/D = 0.48 s, and radial mixing time is ln100 r^2/D = 0.037 min. Skeletal muscle capillary tissue unit length (x) = 0.1 cm, and mean capillary blood velocity (v) = 0.05 cm/s (16, 27). The time constant for axial diffusion of nitrogen is x^2/D = 769 s, and the time constant for capillary perfusion is x/v = 2 s. Axial mixing is dominated by capillary perfusion, and that mixing time is ln100 x/v = 0.15 min. Both radial and axial mixing times are an order or more of magnitude smaller than the fastest time constant for flow into and out of any hind limb model compartment: V_{ven}/Q = 2.7 min (countercurrent model, combined nitrogen and helium hind limb parameter estimates, high blood flow state). Other hind limb time constants are one to two orders of magnitude larger, indicating that consideration of concentration gradients across capillary tissue units is not relevant to the time course of the present studies and the well-mixed assumption is appropriate.

Fit of all the structural models of the hind limb to the nitrogen data alone resulted in estimated compartment volumes about 25% smaller than those estimated by fit to the helium data alone. This difference in compartment apparent volumes (V_1, V_2, V_{tot}) can be partially accounted for by the use of a

unity partition coefficient for both gases; the apparent volume is equal to the true volume times the partition coefficient. Published solubility coefficients for nitrogen and helium, all in species other than sheep (22), indicate a helium partition coefficient between muscle and blood of about 1.18 and a nitrogen partition coefficient between brain and blood of about 1.06. The difference between these latter values and unity accounts for only about a 10% difference in hind limb apparent volume estimates. It is possible the remaining difference in apparent volumes for the two gases may be due to loss of helium from the system, but models that include a term for loss of helium were not justified by the data (data not shown). The remaining differences in estimated apparent volumes for the two gases indicates slower kinetics of helium than nitrogen in the hind limb. Such a difference may not be truly resolvable by fit of the structural models to the mean data. Indeed, models with the same volume estimates for the two gases, and therefore the same kinetics, fit the data well.

These findings have implications for decompression algorithms. The majority of decompression algorithms model the kinetics of inert gases in a collection of compartments with different time constants spanning the range of tissue kinetics relevant to decompression sickness. Decompression algorithms that accommodate multiple gases may assign different time constants to nitrogen and helium for the same compartment. This structure is appropriate for compartments with slow gas exchange, as evidenced by slower whole-body washout of nitrogen than of helium (3, 14). This slower washout of nitrogen than helium from tissues with slow gas exchange probably underlies the slower required decompression from nitrogen-oxygen than from helium-oxygen saturation dives (15). Saturation dives are hyperbaric exposures of sufficient duration that all body tissues have equilibrated with inspired inert gas partial pressure, and the slowest washout of gas from tissues limits the rate of decompression from such dives. However, some decompression algorithms assign faster time constants for helium than for nitrogen in all compartments (6). The present findings indicate this latter structure is not appropriate because nitrogen and helium exchange at similar rates in some tissues. For the best of the present models, the slowest compartment time constant for a normal blood flow state was $V_1/Q = 24$ min (countercurrent model, combined nitrogen and helium hind limb parameter estimates), which is relatively fast in terms of the collection of time constants used in decompression algorithms. The extent of gas uptake into compartments with fast time constants determines the deepest required decompression stop for dives of insufficient duration for all body tissues to reach equilibration with inspired inert gas partial pressure (bounce dives). A deeper first decompression stop results in longer total decompression time. In model structures with faster helium than nitrogen uptake into fast compartments, a deeper first decompression stop and longer total decompression results from a helium-oxygen bounce dive than from a nitrogen-oxygen bounce dive to the same depth for the same bottom time. This behavior may be inappropriate, but few data exist that directly compare the decompression obligation resulting for helium-oxygen and nitrogen-oxygen bounce dives of identical depth and duration.

In summary, this is the first report of mass mass-balanced, kinetic data for isobaric tissue exchange of nitrogen and helium. In both the brain and hind limb of sheep, the blood:tissue exchange of nitrogen is similar to that of helium. These kinetics are best described by two exponential processes, possibly as a consequence of arterial-venous shunt of these highly diffusible solutes.

ACKNOWLEDGMENTS

We thank A. Martinez for technical assistance. The Australian Centre for Pharmacometrics is an initiative of the Australian Government as part of the National Collaborative Research Infrastructure Strategy.

GRANTS

This work was conducted in part while Dr. Doolette was a Jean B. Reid Medical Research Associate, Health Science Research Committee, the University of Adelaide. Partial support for this study was provided by National Health and Medical Research Council of Australia Grant 970067 (Pharmacokinetics of gases: development of integrated experimental and modeling methods). Partial support for this study was also provided by the University of Adelaide Division of Health Sciences Research Committee.

DISCLOSURES

No conflicts of interest, financial or otherwise, are declared by the author(s).

AUTHOR CONTRIBUTIONS

D.J.D. and R.N.U. conception and design of research; D.J.D., R.N.U., and C.G. performed experiments; D.J.D. and C.G. analyzed data; D.J.D. and R.N.U. interpreted results of experiments; D.J.D. prepared figures; D.J.D. drafted manuscript; D.J.D., R.N.U., and C.G. edited and revised manuscript; D.J.D., R.N.U., and C.G. approved final version of manuscript.

REFERENCES

1. **Ackles KN, Holness DE, Scott CA.** Measurement of uptake and elimination of nitrogen in tissue, in vivo. In: *Underwater Physiology V*, edited by Lambertsen CJ. Bethesda, MD: Federation of American Societies for Experimental Biology, 1976.
2. **Aukland K, Akre S, Leraand S.** Arteriovenous counter-current exchange of hydrogen gas in skeletal muscle. *Scand J Clin Lab Invest Suppl* 99: 72–75, 1967.
3. **Behnke AR, Willmon TL.** Gaseous nitrogen and helium elimination from the body during rest and exercise. *Am J Physiol* 131: 619–626, 1940.
4. **Bell AW, Hales JR, King RB, Fawcett AA.** Influence of heat stress on exercise-induced changes in regional blood flow in sheep. *J Appl Physiol* 55: 1916–1923, 1983.
5. **Brodersen P, Sejrsen P, Lassen NA.** Diffusion bypass of xenon in brain circulation. *Circ Res* 32: 363–369, 1973.
6. **Bühlmann AA.** Experimentalle Grundlagen der risikoarmen Dekompression nach Überdruckexpositionen. *Schweiz Med Wochenschr* 112: 48–59, 1982.
7. **Byrne GD, Hindmarsh AC, Jackson KR, Brown HG.** A comparison of two ODE codes: GEAR and EPISODE. *Comput Chem Eng* 1: 133–147, 1977.
8. **Campbell JA, Hill L.** Studies in the saturation of the tissues with gaseous nitrogen. I. Rate of saturation of goat's bone marrow in vivo with nitrogen during exposure to increased atmospheric pressure. *Q J Exp Biol* 23: 197–210, 1933.
9. **Doolette DJ, Upton RN, Grant C.** Diffusion limited, but not perfusion limited, compartmental models describe cerebral nitrous oxide kinetics at both high and low cerebral blood flows. *J Pharmacokinet Biopharm* 26: 649–672, 1998.
10. **Doolette DJ, Upton RN, Grant C.** Agreement between ultrasonic Doppler venous outflow and Kety-Schmidt estimates of cerebral blood flow. *Clin Exp Pharmacol Physiol* 26: 736–740, 1999.
11. **Doolette DJ, Upton RN, Grant C.** Countercurrent compartmental models describe hind limb skeletal muscle helium kinetics at resting and low blood flows in sheep. *Acta Physiol Scand* 185: 109–121, 2005.
12. **Doolette DJ, Upton RN, Grant C.** Perfusion-diffusion compartmental models describe cerebral helium kinetics at high and low cerebral blood flows in sheep. *J Physiol* 563: 529–539, 2005.
13. **Doolette DJ, Upton RN, Zheng D.** Diffusion-limited tissue equilibration and arteriovenous diffusion shunt describe skeletal muscle nitrous oxide

kinetics at high and low blood flows in sheep. *Acta Physiol Scand* 172: 167–177, 2001.
14. **Duffner GJ, Snider HH.** *Effects of exposing men to compressed air and helium-oxygen mixtures for 12 hours at pressures of 2–2.6 atmospheres* (Research Report 1–59). Panama City, FL: Navy Experimental Diving Unit, 1958.
15. **Eckenhoff RG, Vann RD.** Air and nitrox saturation decompression: a report of 4 schedules and 77 subjects. *Undersea Biomed Res* 12: 41–52, 1985.
16. **Eriksson E, Myrhage R.** Microvascular dimensions and blood flow in skeletal muscle. *Acta Physiol Scand* 86: 211–222, 1972.
17. **Hales JR.** Effect of exposure to hot environments on total and regional blood flow in the brain and spinal cord of the sheep. *Pflugers Arch* 344: 327–337, 1973.
18. **Iversen PO, Standa M, Nicolaysen G.** Marked regional heterogeneity in blood flow within a single skeletal muscle at rest and during exercise hyperaemia in the rabbit. *Acta Physiol Scand* 136: 17–28, 1989.
19. **Kety SS, Schmidt CF.** The determination of cerebral blood flow in man by the use of nitrous oxide in low concentrations. *Am J Physiol* 143: 51–66, 1945.
20. **Kjellmer I, Lindberg I, Prerovsky I, Tønnesen H.** The relation between blood flow in an isolated muscle measured with the Xe^{133} clearance and a direct recording technique. *Acta Physiol Scand* 69: 69–78, 1967.
21. **Klein B, Kuschinsky W, Schrock H, Vetterlein F.** Interdependency of local capillary density, blood flow, and metabolism in rat brains. *Am J Physiol Heart Circ Physiol* 251: H1333–H1340, 1986.
22. **Lango T, Morland T, Brubakk AO.** Diffusion coefficients and solubility coefficients for gases in biological fluids: a review. *Undersea Hyperb Med* 23: 247–272, 1996.
22a. **National Health and Medical Research Council.** *Australian Code of Practice for the Care and Use of Animals for Scientific Purposes*, 6th ed. Canberra: Australian Government Publishing Service, 1997.
23. **Novotny JA, Mayers DL, Parsons YF, Survanshi SS, Weathersby PK, Homer LD.** Xenon kinetics in muscle are not explained by a model of parallel perfusion-limited compartments. *J Appl Physiol* 68: 876–890, 1990.
24. **Perl W, Rackow H, Salanitre E, Wolf GL, Epstein RM.** Intertissue diffusion effect for inert fat-soluble gases. *J Appl Physiol* 20: 621–627, 1965.
25. **Piiper J, Meyer M, Scheid P.** Dual role of diffusion in tissue gas exchange: blood-tissue equilibration and diffusion shunt. *Resp Physiol* 56: 131–144, 1984.
26. **Renkin EM.** Control of microcirculation and blood-tissue exchange. In: *Handbook of Physiology. The Cardiovascular System*. Microcirculation. Bethesda, MD: Am. Physiol. Soc., 1984, sect. 2, vol. 4, pt. 2, chapt. 14, p. 627–687.
27. **Schmidt-Nielsen K, Pennycuik P.** Capillary density in mammals in relation to body size and oxygen consumption. *Am J Physiol* 200: 746–750, 1961.
28. **Sejrsen P, Tønnesen KH.** Inert gas diffusion method for measurement of blood flow using saturation techniques. *Circ Res* 22: 679–693, 1968.
29. **Sejrsen P, Tønnesen KH.** Shunting by diffusion of inert gas in skeletal muscle. *Acta Physiol Scand* 86: 82–91, 1972.
30. **Upton RN, Grant C, Ludbrook GL.** An ultrasonic Doppler venous outflow method for the continuous measurement of cerebral blood flow in conscious sheep. *J Cereb Blood Flow Metab* 14: 680–688, 1994.
31. **Zheng D, Doolette DJ, Upton RN.** In vivo manipulation and continuous measurement of muscle blood flow with venous effluent sampling. *Clin Exp Pharmacol Physiol* 27: 625–629, 2000.